Accepted version of the paper: A. Giusti, J. Malzahn, N. G. Tsagarakis and M. Althoff, "On the Combined Inverse-Dynamics/Passivity-Based Control of Elastic-Joint Robots," in IEEE Transactions on Robotics, vol. 34, no. 6, pp. 1461-1471, Dec. 2018, doi: 10.1109/TRO.2018.2861917.

On the Combined Inverse-Dynamics/Passivity-Based Control of Elastic-Joint Robots

Andrea Giusti, Jörn Malzahn, Nikolaos G. Tsagarakis, and Matthias Althoff

***Abstract*—We present a novel global tracking control approach for elastic-joint robots which can be efficiently computed and is robust against model uncertainties and input disturbances. Elastic-joint robots provide enhanced safety and resiliency for interaction with the environment and humans. On the other hand, the joint elasticity complicates the motion-control problem especially when robust and precise trajectory tracking is required. Our proposed control approach allows us to merge the main benefits of two well-known control schemes: inverse-dynamics control, which can be efficiently computed thanks to modern recursive algorithms, and passivity-based tracking control, which provides enhanced robustness to model uncertainty and external disturbances. As an extension of our previous work, we present a detailed robustness analysis of our combined Inverse-Dynamics/Passivity-Based controller, a new variant of the original scheme which shows practically relevant implications, and finally, experimental results which verify the effectiveness of the approach.**

***Index Terms*—Elastic-joint robots, motion control, inverse-dynamics control, passivity-based control**

I. Introduction

MODERN advanced robotic applications benefit from resilient, compliant robots that can provide safe and dependable interaction with humans and the environment [1]. These systems have enjoyed growing interest in recent decades, in particular towards the intentional inclusion of elastic elements in the structures of robots [2]. In fact, a typical means of adding compliance to a robotic structure is the use of elastic elements in the joints e.g., by using series elastic actuators [3], [4]. However, in such cases motion control is significantly more complex with respect to the classical rigid case due to the necessary extension of the state variables to capture both motor-side and link-side dynamics, coupled through elastic elements.

The control problem of elastic-joint robots has attracted numerous researchers since the mid '80s. Fundamental works up to the mid '90s are summarized and detailed in [6], [7], while more recent results have been collected in [2], [8]. One of the most celebrated results is the model reduction approach by [9], which is based on very reasonable assumptions. This result makes the control problem significantly more tractable with respect to the use of a complete model from the classical Lagrangian formulation, enabling the realization of static feedback-linearizing controllers for trajectory tracking. This additionally paved the way for the development of control laws based on the singular perturbation technique, which can be found in [10]. This approach has shown to be very effective when sufficiently high stiffness is present in the joints, as described in the experimental comparison with the feedback-linearizing controller on a single-link arm in [11]. A practical solution for trajectory tracking has been introduced in [12], where the authors propose an effective feedforward/feedback method for which local stability can be shown [13]. A semi-global tracking controller for elastic-joint robots, which interestingly does not require the calculation of the link jerks, can be found in [14]. A comparative study of global tracking controllers based on decoupling, backstepping, and passivity is presented in [15]. Among more recent works, an approach for trajectory tracking where limited sensing capability is considered for lossless elastic-joint manipulators can be found in [16], [17], and a passivity-based approach for both link-

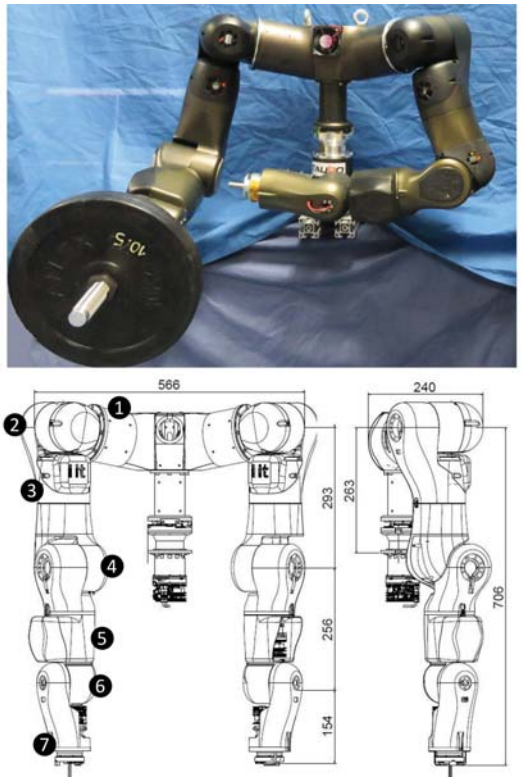

Fig. 1. Picture (*top*) and dimensions in *mm* (*bottom*) of the bi-manual robotic platform [5] serving for the experimental evaluation of the proposed controller.

A. Giusti is with the team of Automation and Mechatronics, Fraunhofer Italia Research, Bolzano, 39100, Italy, e-mail: andrea.giusti@fraunhofer.it.

J. Malzahn and N.G. Tsagarakis are with the Department of Advanced Robotics, (Fondazione) Istituto Italiano di Tecnologia, e-mail: {jorn.malzahn, nikos.tsagarakis}@iit.it.

M. Althoff is with the Department of Informatics, Technical University of Munich (TUM), Garching, 85748, Germany, e-mail: matthias.althoff@tum.de.

Manuscript received Month DD, YYYY; revised Month DD, YYYY.

side tracking and damping assignment considering nonlinear springs is presented in [18]. Effective approaches that focus on the regulation control problem are reported e.g., by [19]–[21].

In this paper, we focus on the global tracking control problem. Among the existing methods, the inverse-dynamics control scheme is especially attractive thanks to recently proposed algorithms that allow its efficient implementation such as in [22], [23]. However, this controller relies on the exact cancellation of the system couplings and may be sensitive to even small model mismatches, as shown by simulations in [24]. Also, other authors have previously realized the risk of poor robustness of such a control technique, such as in [15], among others. The authors of [15] suggest an effective passivity-based controller as an alternative. On the other hand, an algorithm for a computationally efficient implementation of passivity-based controllers for global tracking of elastic-joint robots (e.g., [15], [18]) is not yet available to the best of our knowledge as is the case for inverse-dynamics control.

In this work, we present a control scheme that provides enchanced robustness to model uncertainties and external disturbances, which can still be computed in the same computationally efficient way as classical inverse-dynamics control schemes can. Our new global tracking control approach is based on the partial cancellation of the modeled system dynamics, combined with the exploitation of the passivity-related properties of the robot model. Our proposed combined Inverse-Dynamics/Passivity-Based (ID/PB) control scheme allows us to merge the enhanced robustness typical of passivity-based controllers (see e.g., [25]–[27]) with the efficient numerical computability recently made possible for inverse-dynamics control of elastic-joint robots in [22], [23], [28]. This paper extends our previous work in [24] to provide: *1)* a detailed robustness analysis with respect to model uncertainties and external disturbances, *2)* a new variant of the proposed controller which includes a feedforward inverse-dynamics action showing practically relevant implications, and *3)* experimental results on a 7-degrees-of-freedom arm with mixed rigid/elastic joints.

In the next section we detail the control problem. In section III we present the complete control approach with its detailed robustness analysis. We show experimental results in section IV, to draw the conclusion in section V.

II. Control Problem

We focus on the global tracking control problem of robot manipulators composed of N links serially connected through elastic joints and adopt "Spong's assumptions" [9]. We redirect the reader to that work for a detailed description of these assumptions which are, however, justifiable for the large class of robots with high gear ratios. We consider the following model:

$$\mathbf{M}(\mathbf{q})\ddot{\mathbf{q}} + \mathbf{n}(\mathbf{q},\dot{\mathbf{q}}) + \mathbf{K}(\mathbf{q}-\theta) = \tau_{ext}, \tag{1a}$$

$$\mathbf{J}\ddot{\theta} + \mathbf{f}(\dot{\theta}) + \underbrace{\mathbf{K}(\theta-\mathbf{q})}_{:=\tau_e} = \mathbf{u}, \tag{1b}$$

where $\mathbf{q} \in \mathbb{R}^N$ is the vector of link-side joint position variables, $\theta \in \mathbb{R}^N$ is the vector of motor-side joint position variables, $\mathbf{M}(\mathbf{q}) \in \mathbb{R}^{N\times N}$ is the inertia matrix of the rigid links assembly, $\mathbf{J} \in \mathbb{R}^{N\times N}$ is the constant diagonal matrix of the rotor inertia moments through the square of the respective gear ratio, $\mathbf{K} \in \mathbb{R}^{N\times N}$ is the diagonal joint stiffness matrix, $\mathbf{u} \in \mathbb{R}^N$ is the vector of control input forces/torques, $\mathbf{f}(\dot{\theta}) \in \mathbb{R}^N$ is the vector of the motor-side friction terms, $\tau_e \in \mathbb{R}^N$ is the elastic torque vector, and $\tau_{ext} \in \mathbb{R}^N$ is the vector of external forces applied to the manipulator mapped onto the joint space. The centrifugal, Coriolis, gravitational, and link side friction contributions are collected in the following term:

$$\mathbf{n}(\mathbf{q},\dot{\mathbf{q}}) = \mathbf{C}(\mathbf{q},\dot{\mathbf{q}})\dot{\mathbf{q}} + \mathbf{D}\dot{\mathbf{q}} + \mathbf{g}(\mathbf{q}), \tag{2}$$

where $\mathbf{g}(\mathbf{q}) \in \mathbb{R}^N$ is the vector of the gravity terms, $\mathbf{D} \in \mathbb{R}^{N\times N}$ is the matrix of the link-side viscous damping coefficients, and $\mathbf{C}(\mathbf{q},\dot{\mathbf{q}})\dot{\mathbf{q}} \in \mathbb{R}^N$ is the vector of Coriolis and centrifugal terms, with $\mathbf{C}(\mathbf{q},\dot{\mathbf{q}}) \in \mathbb{R}^{N\times N}$ being a matrix such that the following holds:

$$\mathbf{x}^T\left(\dot{\mathbf{M}}(\mathbf{q},\dot{\mathbf{q}}) - 2\,\mathbf{C}(\mathbf{q},\dot{\mathbf{q}})\right)\mathbf{x} = \mathbf{0}, \quad \forall \mathbf{x} \in \mathbb{R}^N. \tag{3}$$

For the scenario described above, we provide a controller which is able to globally track link-side joint-space trajectories $\mathbf{q}_d(t)$, which are at least four times differentiable:

$$\lim_{t\to\infty} \|\underbrace{\mathbf{q}(t) - \mathbf{q}_d(t)}_{:=\mathbf{e}(t)}\| = 0.^1$$

When significant model uncertainties and disturbances are present, we consider a more practical stability target to ensure ultimate boundedness of the trajectories. More precisely, we seek

$$\|\mathbf{q}(t) - \mathbf{q}_d(t)\| < \varepsilon, \ \forall\, t \geq t^*,$$

for a finite positive ε and a finite time t^*.

Except when stressing certain aspects, throughout this paper we adopt two measures to keep the mathematical description succinct: *1)* we omit the time dependence of time-varying variables, and *2)* we additionally omit joint variable dependencies of the model terms. For example, the matrix $\mathbf{M}\big(\mathbf{q}(t)\big)$ will be simply denoted by $\mathbf{M}$, its first derivative over time as $\dot{\mathbf{M}}$ instead of $\dot{\mathbf{M}}\big(\mathbf{q}(t),\dot{\mathbf{q}}(t)\big)$, and its second derivative as $\ddot{\mathbf{M}}$ instead of $\ddot{\mathbf{M}}\big(\mathbf{q}(t),\dot{\mathbf{q}}(t),\ddot{\mathbf{q}}(t)\big)$. The same notation is also employed for the other model terms.

III. Proposed Approach

In this section, we first present the derivation of our proposed combined ID/PB controller as a modification of the classical inverse dynamics controller. Then, we describe a small variant of it, which has been shown to provide improved performance in practice when facing rough estimates of feedback variables. The description of these two control laws is followed by a way to efficiently implement them using off-the-shelf recursive numerical algorithms. A detailed analysis of the robustness with respect to model mismatches and external disturbances completes the section.

[1] All the norms of vectors in this paper are Euclidean norms, while all norms of matrices are induced 2-norms.

A. Combined ID/PB Control

The basic idea of our proposed control law is that (contrary to classical inverse-dynamics control) we do not require the perfect cancellation of nonlinear coupling model terms through feedback. In fact, we perform only a partial cancellation of the couplings to resort to passivity-based control principles to ensure stability and performance.

To formulate a clear description of the controller derivation, we proceed as for the classical inverse-dynamics controller. From the model in (1), we consider availability of measurements of joint positions and velocities for both the link and the motor side, and we assume (for now) that no external forces are applied to the robot i.e., $\tau_{ext} = \mathbf{0}$. In this case, by rearranging (1a), differentiating it twice, and using the notation of $\mathbf{x}^{[n]}$ for denoting $\frac{d^n}{dt^n}\mathbf{x}$ with $n \in \{3,4\}$, the following relation can be obtained:

$$\ddot{\theta} = \mathbf{K}^{-1}\big(\mathbf{M}\mathbf{q}^{[4]} + 2\dot{\mathbf{M}}\mathbf{q}^{[3]} + \ddot{\mathbf{M}}\ddot{\mathbf{q}} + \ddot{\mathbf{n}}\big) + \ddot{\mathbf{q}}, \tag{4}$$

where

$$\ddot{\mathbf{n}} = (\mathbf{C}+\mathbf{D})\,\mathbf{q}^{[3]} + \ddot{\mathbf{C}}\dot{\mathbf{q}} + 2\dot{\mathbf{C}}\ddot{\mathbf{q}} + \dddot{\mathbf{g}}. \tag{5}$$

On the other hand (by considering the definition of τ_e in (1b)), one can rewrite (1a) as

$$\mathbf{M}(\mathbf{q})\ddot{\mathbf{q}} + \mathbf{n}(\mathbf{q},\dot{\mathbf{q}}) = \tau_e. \tag{6}$$

Now, by substituting (4) and (6) in (1b), we obtain

$$\mathbf{J}\mathbf{K}^{-1}\big(\mathbf{M}\mathbf{q}^{[4]} + 2\dot{\mathbf{M}}\mathbf{q}^{[3]} + \ddot{\mathbf{M}}\ddot{\mathbf{q}} + \ddot{\mathbf{n}}\big) + \big(\mathbf{M}+\mathbf{J}\big)\ddot{\mathbf{q}} + \mathbf{n} + \mathbf{f} = \mathbf{u}. \tag{7}$$

From the position of (7), by considering an auxiliary control input vector $\mathbf{y}$, it is not difficult to see that the use of the following classical inverse-dynamics control scheme

$$\mathbf{u}_{ID} = \mathbf{J}\mathbf{K}^{-1}\big(\mathbf{M}\mathbf{y} + 2\dot{\mathbf{M}}\mathbf{q}^{[3]} + \ddot{\mathbf{M}}\ddot{\mathbf{q}} + \ddot{\mathbf{n}}\big) + \big(\mathbf{M}+\mathbf{J}\big)\ddot{\mathbf{q}} + \mathbf{n} + \mathbf{f}, \tag{8}$$

allows one to obtain a linear and decoupled system: $\mathbf{q}^{[4]} = \mathbf{y}$. From here, the designer can assign an asymptotically stable dynamics of the tracking error through $\mathbf{y}$ to complete the classical inverse-dynamics control law.

The derivation of our proposed controller can now be seen as a modification of (8). In fact, from this position we expand $\ddot{\mathbf{n}}$ in (8) using (5), we remove the model terms $\mathbf{M}\mathbf{y}$ and $\mathbf{C}\mathbf{q}^{[3]}$, and we include a new auxiliary vector ν to obtain

$$\mathbf{u}_{IDPB} = \mathbf{J}\mathbf{K}^{-1}\big(2\dot{\mathbf{M}}\mathbf{q}^{[3]} + \ddot{\mathbf{M}}\ddot{\mathbf{q}} + \mathbf{D}\mathbf{q}^{[3]} + \ddot{\mathbf{C}}\dot{\mathbf{q}} + 2\dot{\mathbf{C}}\ddot{\mathbf{q}} + \dddot{\mathbf{g}}\big) + \big(\mathbf{M}+\mathbf{J}\big)\ddot{\mathbf{q}} + \mathbf{n} + \mathbf{f} + \nu. \tag{9}$$

By applying (9) to (7), we avoid the complete cancellation of the overall system dynamics. We do not reach a linear decoupled system and instead obtain

$$\mathbf{J}\mathbf{K}^{-1}\big(\mathbf{M}\mathbf{q}^{[4]} + \mathbf{C}\mathbf{q}^{[3]}\big) = \nu. \tag{10}$$

We can now complete the control law using

$$\nu = -\mathbf{J}\mathbf{K}^{-1}\big(\mathbf{M}\mathbf{q}_a^{[4]} + \mathbf{C}\mathbf{q}_a^{[3]} + \Lambda\mathbf{r}\big), \tag{11}$$

where Λ is any positive definite matrix of proper dimensions and

$$\begin{aligned}\mathbf{r} &= \mathbf{e}^{[3]} + \mathbf{K}_{CB3}\ddot{\mathbf{e}} + \mathbf{K}_{CB2}\dot{\mathbf{e}} + \mathbf{K}_{CB1}\,\mathbf{e},\\ \mathbf{q}_a^{[3]} &= -\mathbf{q}_d^{[3]} + \mathbf{K}_{CB3}\ddot{\mathbf{e}} + \mathbf{K}_{CB2}\dot{\mathbf{e}} + \mathbf{K}_{CB1}\,\mathbf{e},\\ \mathbf{q}_a^{[4]} &= -\mathbf{q}_d^{[4]} + \mathbf{K}_{CB3}\mathbf{e}^{[3]} + \mathbf{K}_{CB2}\ddot{\mathbf{e}} + \mathbf{K}_{CB1}\,\dot{\mathbf{e}}.\end{aligned} \tag{12}$$

By applying our proposed control law in (9) with (11) to the system in (7), we obtain the following closed-loop relation

$$\mathbf{M}\dot{\mathbf{r}} + \mathbf{C}\mathbf{r} + \Lambda\mathbf{r} = \mathbf{0}. \tag{13}$$

Since no perturbation is assumed so far, the right-hand side of (13) is zero; this allows us to conclude that $\mathbf{r}$ will globally and asymptotically converge to zero, as theoretically supported from the large body of literature on passivity-based control (see e.g., [29], [30]). The convergence to zero of the tracking error directly follows, provided that the diagonal gain matrices $\mathbf{K}_{CB3}$, $\mathbf{K}_{CB2}$, and $\mathbf{K}_{CB1}$ are properly selected. The jth element of the diagonal of these matrices for $i \in \{1,2,3\}$ is denoted by $\mathbf{K}_{CBi_{jj}}$; we choose the gains such that the following polynomials are Hurwitz:

$$cb_j(x) := x^3 + K_{CB3_{jj}}x^2 + K_{CB2_{jj}}x + K_{CB1_{jj}},\ \ \forall j \in \{1,\dots N\}.$$

This requirement can be seen more clearly by applying the Laplace transform to the jth coordinate of (12) (using the Laplace variable s) and considering the transfer function from $r_j(s)$ to $e_j(s)$:

$$e_j(s) = \frac{1}{s^3 + K_{CB3_{jj}}s^2 + K_{CB2_{jj}}s + K_{CB1_{jj}}}\,r_j(s). \tag{14}$$

The stability properties of the closed-loop system can also be analyzed by considering the cascade of subsystems in (12) and (13). Remarkably, this approach lets one infer uniform global exponential stability of the overall closed-loop system. This follows by considering that in (12) the origin of $\mathbf{r}$ is uniformly globally exponentially stable and that the same holds for (13) with $\mathbf{e}$ when $\mathbf{r} \equiv 0$. Thus, by invoking the fundamental results in [31], [32], uniform global exponential stability of the overall closed-loop system follows directly.

As introduced earlier, the measurements required for the practical implementation of our proposed controller are the joint positions and joint velocities, both for the link and the motor sides. Even if our proposed controller (as is the case for the classical inverse-dynamics control scheme) requires the feedback of link-side joint accelerations and jerks, one can, in principle, obtain them by exploiting the model knowledge with the following relations:[2]

$$\ddot{\mathbf{q}} = \mathbf{M}^{-1}\big(\tau_e - \mathbf{n}\big), \tag{15}$$

$$\mathbf{q}^{[3]} = \mathbf{M}^{-1}\Big(\dot{\tau}_e - \big(\dot{\mathbf{M}}\ddot{\mathbf{q}} + \dot{\mathbf{n}}\big)\Big). \tag{16}$$

[2]It is important to mention that in the more general case of $\tau_{ext} \neq \mathbf{0}$, one should also include such contribution and thus require availability of corresponding sensors.

B. Combined ffwd-ID/PB Control

Even though the above mentioned approach for estimating joint accelerations and jerks is certainly viable in principle, the accuracy of the corresponding estimates can be poor in practice. In fact, this is the case when noisy/biased torque readings are available for lightweight robotic structures and/or when the knowledge of the model is not sufficiently precise. An alternative to estimating these quantities can rely on the use of an observer, e.g., as in [24] when the model knowledge is considered accurate but the torque readings are noisy. Instead, when the model knowledge is poor and one faces significant systematic errors of the acceleration estimates, one can resort to using a kinematic-Kalman-filter-based approach as in [33].

Our proposed controller relies on the partial cancellation of nonlinear coupling terms through feedback. Such terms should be computed using the estimates of accelerations and jerks. Poor/delayed estimates are a source of direct perturbation injected by the controller, which affects the control performance directly. We foster a practical solution based on feedforward control for the inverse-dynamics part of our controller to provide a combined feedforward-ID/PB scheme:

$$\mathbf{u}_{ffwdIDPB} = \mathbf{u}_{d,ID}(\mathbf{q}_d, \dot{\mathbf{q}}_d, \ddot{\mathbf{q}}_d, \mathbf{q}_d^{[3]}) + \mathbf{f}(\dot{\theta}) - \mathbf{J}\mathbf{K}^{-1}\big(\mathbf{M}(\mathbf{q})\,\mathbf{q}_a^{[4]} + \mathbf{C}(\mathbf{q},\dot{\mathbf{q}})\,\mathbf{q}_a^{[3]} + \Lambda\mathbf{r}\big), \quad (17)$$

where

$$\mathbf{u}_{d,ID}(\mathbf{q}_d, \dot{\mathbf{q}}_d, \ddot{\mathbf{q}}_d, \mathbf{q}_d^{[3]}) = \mathbf{J}\mathbf{K}^{-1}\Big(2\dot{\mathbf{M}}_d\,\mathbf{q}_d^{[3]} + \ddot{\mathbf{M}}_d\,\ddot{\mathbf{q}}_d + \mathbf{D}\,\mathbf{q}_d^{[3]} + \ddot{\mathbf{C}}_d\dot{\mathbf{q}}_d + 2\,\dot{\mathbf{C}}_d\ddot{\mathbf{q}}_d + \ddot{\mathbf{g}}_d\Big) + \big(\mathbf{M}_d + \mathbf{J}\big)\ddot{\mathbf{q}}_d + \mathbf{n}_d.$$

For compactness, in the above equation we denote with the subscript d the model terms that are evaluated along the desired trajectory. For example, we denote the model term $\dot{\mathbf{M}}(\mathbf{q}_d(t), \dot{\mathbf{q}}_d(t))$ simply by $\dot{\mathbf{M}}_d$. The effectiveness of the combined feedforward-ID/PB control law has been verified by experiments, as shown in Section IV.

C. Efficient Computation of the Proposed Controllers

A particularly interesting aspect of our proposed control laws compared to most existing passivity-based tracking schemes resides in its straightforward and efficient implementability, that is, using a combination of modern recursive algorithms for robot dynamics computation. In particular, let us first denote with EJNEA (Elastic Joint Newton-Euler Algorithm) the algorithm for efficiently computing the inverse dynamics of robots with elastic joints as recently proposed in [22], [28], which yields

$$\mathbf{J}\mathbf{K}^{-1}\Big[\mathbf{M}\mathbf{q}^{[4]} + 2\dot{\mathbf{M}}\mathbf{q}^{[3]} + \ddot{\mathbf{M}}\ddot{\mathbf{q}} + \ddot{\mathbf{n}}\Big] + [\mathbf{M}+\mathbf{J}]\ddot{\mathbf{q}} + \mathbf{n} = \mathrm{EJNEA}(\mathbf{q}, \dot{\mathbf{q}}, \ddot{\mathbf{q}}, \mathbf{q}^{[3]}, \mathbf{q}^{[4]}),$$

and with NE* the well-established algorithm for efficient recursive computation of passivity-based controllers of rigid robots introduced in [25], which yields

$$\mathbf{M}\ddot{\mathbf{q}} + \mathbf{C}\dot{\mathbf{q}}_a = \mathrm{NE}_0^*(\mathbf{q}, \dot{\mathbf{q}}, \dot{\mathbf{q}}_a, \ddot{\mathbf{q}}),$$

when gravity effects are not considered (here denoted by the subscript 0). It is now easy to see that our proposed combined ID/PB control law can be efficiently implemented as follows:

$$\mathbf{u}_{IDPB} = \mathrm{EJNEA}(\mathbf{q}, \dot{\mathbf{q}}, \ddot{\mathbf{q}}, \mathbf{q}^{[3]}, \mathbf{0}) - \mathbf{J}\mathbf{K}^{-1}\big(\mathrm{NE}_0^*(\mathbf{q}, \dot{\mathbf{q}}, \underbrace{\mathbf{q}_a^{[3]} + \mathbf{q}^{[3]}}_{=\mathbf{r}}, \mathbf{q}_a^{[4]}) + \Lambda\mathbf{r}\big) + \mathbf{f}(\dot{\theta}). \quad (18)$$

Consequently, its variant with feedforward action simply becomes

$$\mathbf{u}_{ffwdIDPB} = \mathrm{EJNEA}(\mathbf{q}_d, \dot{\mathbf{q}}_d, \ddot{\mathbf{q}}_d, \mathbf{q}_d^{[3]}, \mathbf{0}) - \mathbf{J}\mathbf{K}^{-1}\big(\mathrm{NE}_0^*(\mathbf{q}, \dot{\mathbf{q}}, \underbrace{\mathbf{q}_a^{[3]} + \mathbf{q}^{[3]}}_{=\mathbf{r}}, \mathbf{q}_a^{[4]}) + \Lambda\mathbf{r}\big) + \mathbf{f}(\dot{\theta}). \quad (19)$$

Both recalled algorithms (*EJNEA* and *NE**) have linear computational complexity and can be directly used for online numerical computations. Our proposed control laws inherit these features in light of (18) and (19), since two algorithms with linear computational complexity are called once for each sample when running online. In contrast, many other passivity-based global tracking controllers for elastic joint robots (e.g., [15], [18]) require one to obtain the first and second derivative of the matrices $\mathbf{M}$, $\mathbf{C}$ that fulfill (3). To the best knowledge of the authors, no algorithm exists yet for such obtainment with linear computational complexity. Instead, with our proposed schemes, the contributions of $\ddot{\mathbf{M}}$, $\ddot{\mathbf{C}}$, $\dot{\mathbf{M}}$, and $\dot{\mathbf{C}}$ can be included within the computations of *EJNEA*, which runs with linear computational complexity.

D. Analysis of Robustness

In this subsection, we consider the more general case in which the external torque vector τ_{ext} (sufficiently smooth) is different from zero and the robot does not have sensors for measuring it. We assume that the model is not perfect and that only nominal model terms are available for feedback control. We denote the nominal model terms with a subscript 0. We use a subscript δ to denote the perturbation from the respective real value. For example, for a generic model term or feedback vector Ξ we can write

$$\Xi = \Xi_0 + \Xi_\delta, \text{ and consequently } \Xi_\delta = \Xi - \Xi_0. \quad (20)$$

Regarding the motor side dynamics, we assume that there is no significant uncertainty in the knowledge of $\mathbf{J}$ and $\mathbf{K}$. This is justified by the fact that in reality such quantities can be precisely estimated during the actuation unit calibration, before the unit is mounted in the robot.

By performing similar algebraic manipulations as in the previous section, it is not difficult to see that for the more general case ($\tau_{ext} \neq 0$), the following relation can be obtained:

$$\mathbf{J}\mathbf{K}^{-1}\Big(\mathbf{M}\mathbf{q}^{[4]} + \mathbf{C}\mathbf{q}^{[3]} + \eta\Big) + \beta = \mathbf{u} + \mathbf{J}\mathbf{K}^{-1}\mathbf{d}, \quad (21)$$

where

$$\eta = 2\dot{\mathbf{M}}\mathbf{q}^{[3]} + \ddot{\mathbf{M}}\ddot{\mathbf{q}} + \mathbf{D}\mathbf{q}^{[3]} + \ddot{\mathbf{C}}\dot{\mathbf{q}} + 2\,\dot{\mathbf{C}}\ddot{\mathbf{q}} + \ddot{\mathbf{g}},$$
$$\beta = \big(\mathbf{M}+\mathbf{J}\big)\ddot{\mathbf{q}} + \mathbf{n} + \mathbf{f}, \quad \text{and} \quad \mathbf{d} = \mathbf{K}\mathbf{J}^{-1}\tau_{ext} + \ddot{\tau}_{ext}.$$

Hereafter, we assume the external torque vector to be sufficiently smooth and bounded so that

$$\|\mathbf{d}\| < \kappa_{\mathbf{d}},$$

for a finite positive $\kappa_{\mathbf{d}}$. The control commands computed with the combined ID/PB control law having only nominal model information can thus be rewritten as follows:

$$\mathbf{u}_{IDPB_0} = \mathbf{J}\mathbf{K}^{-1}\eta_0 + \beta_0 - \mathbf{J}\mathbf{K}^{-1}\big(\mathbf{M}_0\,\mathbf{q}_{a0}^{[4]} + \mathbf{C}_0\,\mathbf{q}_{a0}^{[3]} + \Lambda\mathbf{r}_0\big), \tag{22}$$

where

$$\eta_0 = 2\dot{\mathbf{M}}_0\,\mathbf{q}_0^{[3]} + \ddot{\mathbf{M}}_0\,\ddot{\mathbf{q}}_0 + \mathbf{D}_0\,\mathbf{q}_0^{[3]} + \ddot{\mathbf{C}}_0\dot{\mathbf{q}} + 2\,\dot{\mathbf{C}}_0\ddot{\mathbf{q}}_0 + \ddot{\mathbf{g}}_0,$$
$$\beta_0 = \big(\mathbf{M}_0 + \mathbf{J}\big)\ddot{\mathbf{q}}_0 + \mathbf{n}_0 + \mathbf{f}_0.$$

It is important to notice that the variables that contain acceleration and jerk vectors are also nominal, since either they are estimated in a direct model-based fashion or they are obtained by an observer; their knowledge cannot be considered as perfect for the assumed uncertainty scenario. In fact, the terms used for feedback control are written as

$$\mathbf{r}_0 = \big(\mathbf{q}_0^{[3]} - \mathbf{q}_d^{[3]}\big) + \mathbf{K}_{CB3}\big(\ddot{\mathbf{q}}_0 - \ddot{\mathbf{q}}_d\big) + \mathbf{K}_{CB2}\dot{\mathbf{e}} + \mathbf{K}_{CB1}\,\mathbf{e},$$
$$\mathbf{q}_{a0}^{[3]} = -\mathbf{q}_d^{[3]} + \mathbf{K}_{CB3}\big(\ddot{\mathbf{q}}_0 - \ddot{\mathbf{q}}_d\big) + \mathbf{K}_{CB2}\dot{\mathbf{e}} + \mathbf{K}_{CB1}\,\mathbf{e},$$
$$\mathbf{q}_{a0}^{[4]} = -\mathbf{q}_d^{[4]} + \mathbf{K}_{CB3}\big(\mathbf{q}_0^{[3]} - \mathbf{q}_d^{[3]}\big) + \mathbf{K}_{CB2}\big(\ddot{\mathbf{q}}_0 - \ddot{\mathbf{q}}_d\big) + \mathbf{K}_{CB1}\,\dot{\mathbf{e}}.$$

By using (22) in (21) and after performing long but rather straightforward algebraic manipulations, while keeping (20) in mind, we obtain the following closed-loop relation:

$$\mathbf{M}\dot{\mathbf{r}} + \mathbf{C}\,\mathbf{r} + \Lambda\mathbf{r} = \psi, \tag{23}$$

where

$$\psi = \Lambda\,\mathbf{r}_\delta + \mathbf{M}\mathbf{q}_{a\delta}^{[4]} + \mathbf{C}\,\mathbf{q}_{a\delta}^{[3]} + \mathbf{M}_\delta\mathbf{q}_{a0}^{[4]} + \mathbf{C}_\delta\,\mathbf{q}_{a0}^{[3]} - \eta_\delta - \mathbf{K}\mathbf{J}^{-1}\beta_\delta + \mathbf{d}. \tag{24}$$

In light of (24), we introduce additional assumptions.

Assumption 1: There exist positive constants κ_{M_δ}, κ_{C_δ}, and $\kappa_{\eta\beta_\delta}$ that bound the deviation between the nominal and real model terms (indicated with subscript δ) as follows:

$$\|\mathbf{M}_\delta\| < \kappa_{M_\delta},\quad \|\mathbf{C}_\delta\| < \kappa_{C_\delta},\quad \|\eta_\delta - \mathbf{K}\mathbf{J}^{-1}\beta_\delta\| < \kappa_{\eta\beta_\delta}. \tag{25}$$

This assumption implies that, although the designer does not have perfect knowledge of the model terms, the deviation from the real model (see also (20)) is not expected to be unbounded in practice.[3]

Assumption 2: There exist positive constants $\kappa_{a\delta}$ and $\kappa_{j\delta}$ that bound the deviation between the real and the estimated accelerations and jerks as follows:

$$\|\ddot{\mathbf{q}}_\delta\| < \kappa_{a\delta},\quad \|\mathbf{q}_\delta^{[3]}\| < \kappa_{j\delta}. \tag{26}$$

This is reasonable when considering a well-calibrated estimator of the accelerations and jerks, as well as limitations of real actuators.[4] As a consequence of this assumption, and using the relations

$$\mathbf{q}_{a\delta}^{[4]} \overset{(20)}{=} \mathbf{K}_{CB3}\mathbf{q}_\delta^{[3]} + \mathbf{K}_{CB2}\ddot{\mathbf{q}}_\delta,\ \ \mathbf{q}_{a\delta}^{[3]} \overset{(20)}{=} \mathbf{K}_{CB3}\ddot{\mathbf{q}}_\delta,$$

we can also write that

$$\|\mathbf{q}_{a\delta}^{[4]}\| < \kappa_{as\delta},\quad \|\mathbf{q}_{a\delta}^{[3]}\| < \kappa_{aj\delta}, \tag{27}$$

for some positive constants $\kappa_{as\delta}$ and $\kappa_{aj\delta}$.

Assumption 3: There exist positive constants κ_M and κ_C so that

$$\|\mathbf{M}\| \le \kappa_M \tag{28}$$

and

$$\|\mathbf{C}(\mathbf{q},\dot{\mathbf{q}})\| \le \kappa_C\|\dot{\mathbf{q}}\|. \tag{29}$$

Since this last assumption is more common in the literature on control of robot manipulators, we redirect the reader to related books (e.g., [27]) for further details.

Within the considered uncertainty scenario and the above mentioned assumptions, we can now show that our proposed control scheme allows one to achieve, in principle, any user desired tracking precision, upon proper selection of Λ and the gains $\mathbf{K}_{CB3}$, $\mathbf{K}_{CB2}$, $\mathbf{K}_{CB1}$. We show this by considering the following storage function:

$$V = \frac{1}{2}\mathbf{r}^T\mathbf{M}\mathbf{r},$$

with the derivative

$$\begin{aligned}\dot{V} &\overset{(23)}{=} \mathbf{r}^T(-\mathbf{C}\,\mathbf{r} - \Lambda\mathbf{r} + \psi) + \frac{1}{2}\mathbf{r}^T\dot{\mathbf{M}}\mathbf{r}\\ &\overset{(3)}{=} \mathbf{r}^T\big(-\Lambda\mathbf{r} + \psi\big)\\ &\le -\lambda_{\min}(\Lambda)\,\|\mathbf{r}\|^2 + \|\mathbf{r}\|\|\psi\|,\end{aligned} \tag{30}$$

where $\lambda_{\min}(\Lambda)$ is the minimum eigenvalue of the matrix Λ. Now, we introduce a perturbation bounding function ρ as

$$\rho = \kappa + \kappa_v\|\dot{\mathbf{q}}\| + \kappa_{M_\delta}\|\mathbf{q}_{a0}^{[4]}\| + \kappa_{C_\delta}\|\mathbf{q}_{a0}^{[3]}\| + \varphi_p, \tag{31}$$

where

$$\kappa = \kappa_M\kappa_{as\delta} + \kappa_{\eta\beta_\delta} + \kappa_d,\quad \kappa_v = \kappa_C\kappa_{aj\delta},\quad \varphi_p > 0,$$

and we use it directly for selecting the matrix Λ:

$$\Lambda = \rho\mathbf{I},$$

with $\mathbf{I}$ being the identity matrix of proper dimensions. By considering the assumptions, it can be shown that

$$(1 + \|\mathbf{r}_\delta\|)\rho > \|\psi\|,$$

which allows us to rewrite (30) as

$$\dot{V} < \rho\|\mathbf{r}\|(-\|\mathbf{r}\| + \|\mathbf{r}_\delta\| + 1).$$

From the above inequality we can infer that $\dot{V} < 0$ for

$$\|\mathbf{r}\| \ge \kappa_{j\delta} + \|\mathbf{K}_{CB3}\|\kappa_{a\delta} + 1 \ge \|\mathbf{r}_\delta\| + 1,$$

since

$$\mathbf{r}_\delta \overset{(20)}{=} \mathbf{q}_\delta^{[3]} + \mathbf{K}_{CB3}\ddot{\mathbf{q}}_\delta. \tag{32}$$

[3]This is realistic considering that in real actuators, physical limits ensure bounded velocities.

[4]Assessing boundedness of the error in the estimation of joint accelerations and jerks is a crucial step in any case and must be performed before one uses them for feedback control.

From this result and considering that the inertia matrix (whose minimum and maximum eigenvalues are denoted as $\lambda_m > 0$ and $\lambda_M < \infty$, respectively) is quadratically bounded by

$$\lambda_m \|\mathbf{x}\|^2 \leq \mathbf{x}^T \mathbf{M}\mathbf{x} \leq \lambda_M \|\mathbf{x}\|^2,$$

it can be shown (e.g., *mutatis mutandis* from [34, Theorem 1]) that the trajectories $\mathbf{r}$ are ultimately bounded by

$$\begin{aligned} \|\mathbf{r}\| &\leq (\|\mathbf{r}_\delta\| + 1)\sqrt{\frac{\lambda_M}{\lambda_m}}, \\ &\overset{(32)}{\leq} (\kappa_{j\delta} + \|\mathbf{K}_{CB3}\|\kappa_{a\delta} + 1)\sqrt{\frac{\lambda_M}{\lambda_m}}. \end{aligned} \tag{33}$$

The reader may now realize that there is no direct gain that can be used to shrink the bounds of $\mathbf{r}$. Actually, increasing the gains, and in particular $\mathbf{K}_{CB3}$, enlarges these bounds. The solution is not to focus on shrinking the bounds of $\mathbf{r}$ but on exploiting (14) instead. In fact, for the sake of simplicity, we consider the transfer function in (14) to be the result of a series of first-order low-pass filters[5] for each coordinate j and positive K_G:

$$G_j(s) = \frac{e_j(s)}{r_j(s)} = \frac{1}{(s+K_G)^3} = \frac{1}{s^3 + 3K_G s^2 + 3K_G^2 s + K_G^3},$$

which leads to the gains $\mathbf{K}_{CB3} = 3K_G\mathbf{I}$, $\mathbf{K}_{CB2} = 3K_G^2\mathbf{I}$, and $\mathbf{K}_{CB1} = K_G^3\mathbf{I}$. With this choice and $\|\mathbf{r}\|$ ultimately bounded by (33), we get that for the jth coordinate

$$\begin{aligned} \|e_j\| &\leq \frac{(\kappa_{j\delta} + \|\mathbf{K}_{CB3}\|\kappa_{a\delta} + 1)}{K_G^3}\sqrt{\frac{\lambda_M}{\lambda_m}} \\ &\leq \Big(\frac{(\kappa_{j\delta}+1)}{K_G^3} + \frac{3\kappa_{a\delta}}{K_G^2}\Big)\sqrt{\frac{\lambda_M}{\lambda_m}}, \end{aligned}$$

which shows that the bounds of the tracking error can be made arbitrarily small by selecting a large enough tuning parameter K_G.[6]

IV. Experiments

In this section, we first describe the robot testbed followed by the presentation of three experiments. In particular, we show the tracking performance of the proposed controllers when fast trajectories are required and when significant unknown payload is present. With fast trajectories we refer to trajectories that are fast enough to let us approach (and even reach) the torque/current saturation of actuators during motion. We additionally show how the reduction of the gains affects the performance of our proposed feedforward-ID/PB controller with respect to a simple PD-based scheme, which leads to realizing safer physical human-robot interaction tasks. For all the experiments shown next, the desired trajectories have been computed using 7th order polynomials between point to point motions in joint space. The details of these trajectories can be found in the appendix.

TABLE I
Actuator specifications for one arm. The arms are symmetric and joint indices refer to Fig. 1.

type	gear ratio	joint index	velocity max. [rad/s]	peak torque [Nm]	sensor stiffness [Nm/rad]
Medium A	160	1, 2	5.7	147	6 000
Medium B	160	3, 4	8.2	147	6 000
Small A	100	5, 6	11.6	55	21 000
Small B	100	7	20.3	27	21 000

A. Description of the Robot Testbed

The experimental testbed is the right arm of the bi-manual robotic platform depicted in Fig. 1. The platform has been designed to display human-compatible size, weight, strengths and physical resilience to be capable of both soft interaction as well as harsh manipulation tasks. An in-depth description of the design approach and the platform features are reported in [5].

The specifications of the actuators are listed in Tab. I. The joints with indices 1 to 4 are the first ones in the kinematic chain carrying the highest load. They display a stiffness of $6000\,Nm/rad$. The joints with indices 5 to 7 are subject to lower loads with a stiffness of $21000\,Nm/rad$. This is well in the order of the harmonic gear stiffness at this actuator size and considered rigid for the purpose of this paper.

The arm is therefore a mixed chain of elastic (indices 1 to 4) and rigid (indices 5 to 7) joints, which implies that the dynamics cannot be directly modeled by (1). However, the implementation of our proposed controllers in the presence of mixed rigid/elastic joints is straightforward considering the work in [35]. By following that approach, we create virtual elastic joints for the last three axes of the arm by using dynamic feedback terms in the controller itself. As mentioned in [35], we are able to choose the stiffness and the rotor inertia: here we choose the stiffness to be $100\,Nm/rad$ and the rotor inertia to be $10^{-3}\,kgm^2$. These dynamic feedback terms aim at reproducing elastic-joint motor-side dynamics effects for the rigid axes only, so that our controllers can consider the system as fully composed of elastic joints. The description of the approach we implement for handling mixed rigid/elastic joints exceeds the scope of this paper and we redirect the interested reader to [35] for further details.

The dynamics model computation is carried out online on an Intel NUC with 3 GB DDR-3 RAM and a Core i5-3427U processor (3M cache) running at 1.8 GHz.

B. Validation of the Dynamical Model

Even though the proposed control scheme introduces interesting robustness characteristics to model mismatches as we analyzed in the previous section, its structure is model-based. Therefore, the closer the nominal model is to the real robot dynamics, the better the closed-loop performance is

[5]Please note that in practice other choices of this transfer function can be made, provided that it is stable and sufficiently suppressing (i.e., with sufficiently low H_∞ norm).

[6]Even if we explicated the precise meaning of all bounds considered, we acknowledge that in practice it is difficult to obtain them exactly for properly computing (31). A practical solution is to find from tuning iterations a large enough *constant* ρ that provides satisfactory tracking in conjunction with a large enough K_G.

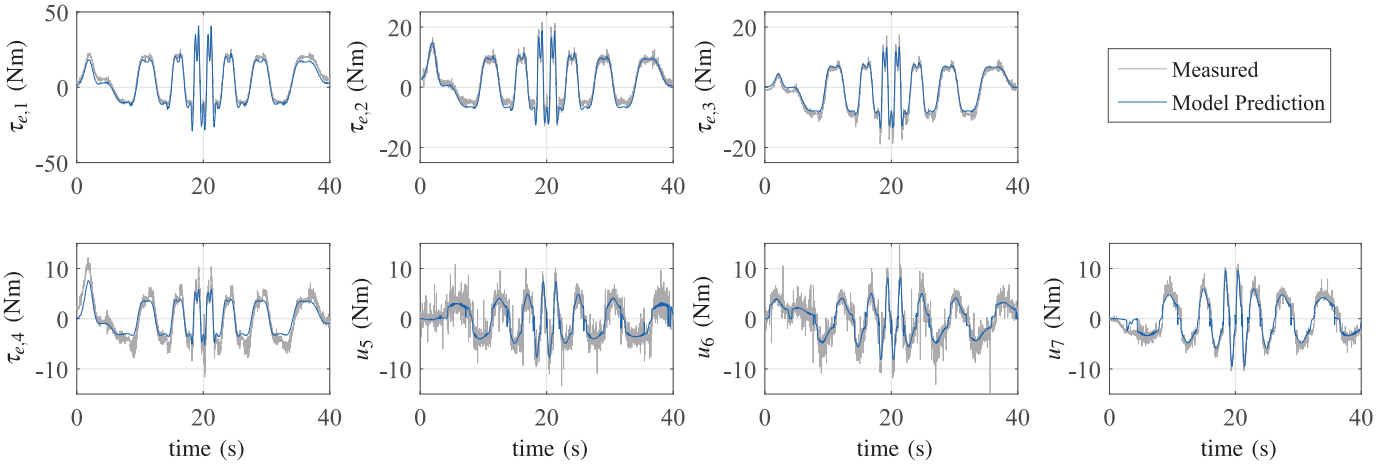

Fig. 2. Evaluation of model accuracy for a closed-loop trajectory tracking control test. The model prediction is computed offline by using the recursive Newton-Euler algorithm for which we use zero-phase digital filtering for estimating the acceleration.

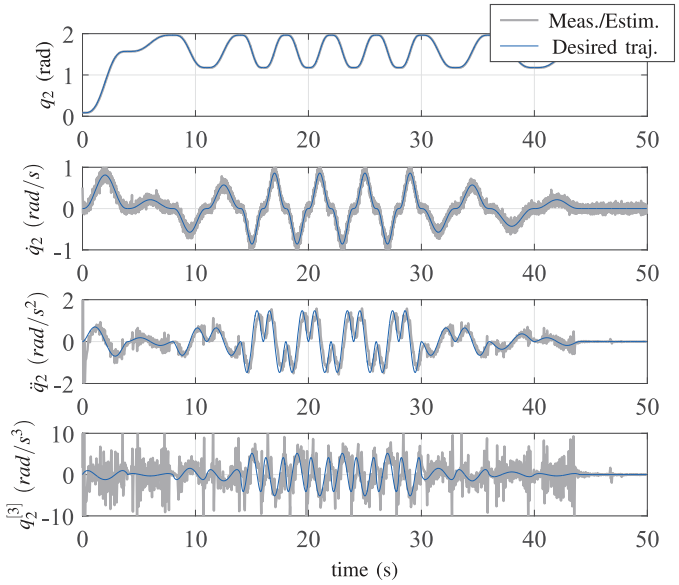

Fig. 3. Example result showing the quality of the estimation of acceleration and jerk for the second axis of the robot while performing a trajectory tracking control test.

under a realistic selection of gains. In our experiments we obtain the nominal model of the rigid-link assembly from CAD data. For the motor side, we use data from the motor data sheets, and we employ a simple identification procedure for obtaining friction estimates as described below. We consider the following simple friction model for the i*th* coordinate of the motor-side dynamics:

$$f_i(\theta_i) = \beta_{v,i}\dot{\theta}_i + \beta_{c,i}\text{sign}(\dot{\theta}_i),$$

where $\beta_{v,i}$ and $\beta_{c,i}$ are the viscous and static friction coefficients, respectively. For obtaining these coefficients, the following regression is performed for the ith axis with an elastic joint and using k samples from a closed-loop identification test

$$[\ \beta_{v,i}\ \ \beta_{c,i}\ ]^T = (\Phi^T\Phi)^{-1}\Phi^T\mathbf{b},$$

where[7]

$$\Phi = \begin{bmatrix} \dot{\theta}_i(1) & \text{sign}(\dot{\theta}_i(1)) \\ \vdots & \vdots \\ \dot{\theta}_i(k) & \text{sign}(\dot{\theta}_i(k)) \end{bmatrix},$$

$$\mathbf{b} = \begin{bmatrix} u_i(1) - \tau_{e,i}(1) - J_i\ddot{\theta}_i(1) \\ \vdots \\ u_i(k) - \tau_{e,i}(k) - J_i\ddot{\theta}_i(k) \end{bmatrix}.$$

The estimation of the friction coefficients of the axes with rigid joints is performed in a similar way by evaluating the model of the rigid-link assembly using a recursive Newton-Euler algorithm in place of the measured τ_e. In all experiments discussed below, the motor-side friction terms have been compensated by feedforward action, using the desired velocity vector. We made this choice to avoid torque flickering from imperfect static friction compensation at low speeds due to noisy velocity readings.

In Fig. 2 we show the results presenting the match of the model derived using CAD data, motor data-sheets, and identified friction coefficients. This figure shows the prediction obtained using the model and the real torque measurements for the axes equipped with elastic joints. Similarly, for the axes with rigid joints, we show the applied actuation torque and compare it with the prediction of the model. From Fig. 2, a reasonably good match can be observed. These results may be improved after performing identification procedures for the dynamic model parameters of the arm (see e.g., [36]–[38]). However, we have not implemented such an approach since one of the purposes of this paper is to show that the proposed controllers provide good performance even if only nominal parameters from CAD data are used.

C. Practical Estimation of Joint Acceleration and Jerk

In practice, torque sensor readings are subject to noise and measurement biases emerging from unmodeled friction in the

[7]The acceleration data have been obtained using zero-phase digital filtering on the double numerical differentiation of the joint position data.

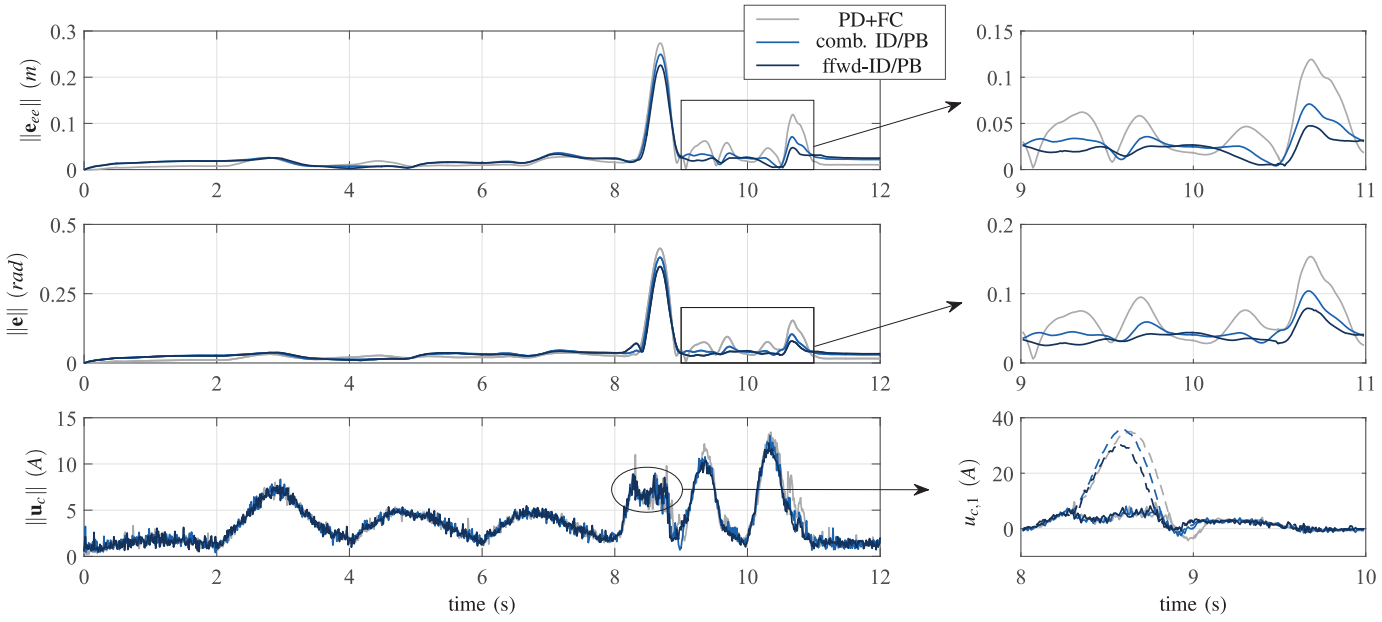

Fig. 4. Experiments of tracking control with fast desired trajectory. The dashed lines in the bottom right plot represent the current commands required from the controllers for the first joint ($u_{c,1}$), where a saturation is experienced. The trajectory used for this test is in the appendix.

link flange support. Together with the model inaccuracies, these effects do not allow us to obtain sufficiently accurate estimates of joint accelerations and jerks using (15) and (16) or to use the observer proposed in [24]. Therefore, we resort to using a simple kinematic Kalman filter with a structure similar to that of [33], using available joint position and velocity readings from the motor. These estimates are additionally filtered by a first-order low-pass filter with cutoff frequency at 5 rad/s for an additional practical suppression of undesired spectral components. For designing the kinematic Kalman filter, we consider the following model:

$$\dot{\mathbf{x}}(t) = \begin{bmatrix} 0 & 1 & 0 & 0 \\ 0 & 0 & 1 & 0 \\ 0 & 0 & 0 & 1 \\ 0 & 0 & 0 & 0 \end{bmatrix} \mathbf{x}(t) + \begin{bmatrix} 0 \\ 0 \\ 0 \\ 1 \end{bmatrix} w(t),$$
$$\mathbf{y}(t) = \begin{bmatrix} 1 & 0 & 0 & 0 \\ 0 & 1 & 0 & 0 \end{bmatrix} \mathbf{x}(t) + \xi(t),$$

where $\mathbf{x}(t) = [q \ \dot{q} \ \ddot{q} \ q^{[3]}]^T$, $\mathbf{y}(t)$ is the vector of the available measurements, $w(t)$ is the unbiased white process noise with a known covariance, and $\xi(t)$ is the vector of unbiased white measurement noise with known covariance matrix. Similar to the considerations made in [39] for $\ddot{q}$, within this model $w(t)$ represents a surrogate of $q^{[4]}$ and its covariance can be considered in practice as a tuning parameter. The results of a test for showing the estimation quality of the acceleration and jerk is presented in Fig. 3. This figure shows the results for the second axis only since the results of the other axes do not differ significantly.

D. Experimental Results

The first experiment we show aims at verifying the tracking performance of the proposed controllers, when no payload is used for fast required trajectories. For this purpose we first present the performance of a PD control with feedforward friction compensation, which results from removing all other model terms as well as the acceleration and jerk feedback from our proposed control law:

$$\mathbf{u}_{PDFC} = -\mathbf{J}\mathbf{K}^{-1}\Lambda(\mathbf{K}_{CB2}\dot{\mathbf{e}} + \mathbf{K}_{CB1}\mathbf{e}) + \mathbf{f}(\dot{\theta}).$$

Next, we introduce the model knowledge and test our proposed combined ID/PB scheme. To complete the test, we include the version of our proposed scheme with the feedforward inverse-dynamics part. The results of this experiment are collected in Fig. 4: the performance provided by the proposed schemes can be clearly noticed by the norm of the tracking error in joint space $\|\mathbf{e}\|$ and in task space $\|\mathbf{e}_{ee}\|$. In particular, the zoomed part of the tracking error plots shows that when the trajectory becomes fast, the combined feedforward-ID/PB control scheme provides the best performance. This is expected since the filtering procedure for cleaning the acceleration and jerk introduces an unavoidable phase lag also noticeable from Fig. 3. It is worth noting that this experiment has been performed in very dynamic conditions for the robot considered, up to its physical actuation limits. This can also be observed from Fig. 4, where the desired actuation current and its saturated execution for the first axis of the robot are shown. This also shows the good behavior of the proposed controllers during and right after actuator saturation. The gains that we used in this experiment are

$$\mathbf{K}_{CB3} = 10^3\text{diag}([60, 120, 120, 120, 2000, 2000, 2000]),$$
$$\mathbf{K}_{CB2} = 10^3\text{diag}([2, 3.5, 3.5, 3.5, 50, 50, 50]),$$
$$\mathbf{K}_{CB1} = \text{diag}([50, 50, 50, 50, 375, 375, 375]),$$
$$\Lambda = \text{diag}([70, 40, 40, 40, 20, 20, 20]).$$

The second experiment shows how unexpected payloads affect the performance of our approach. The results of this

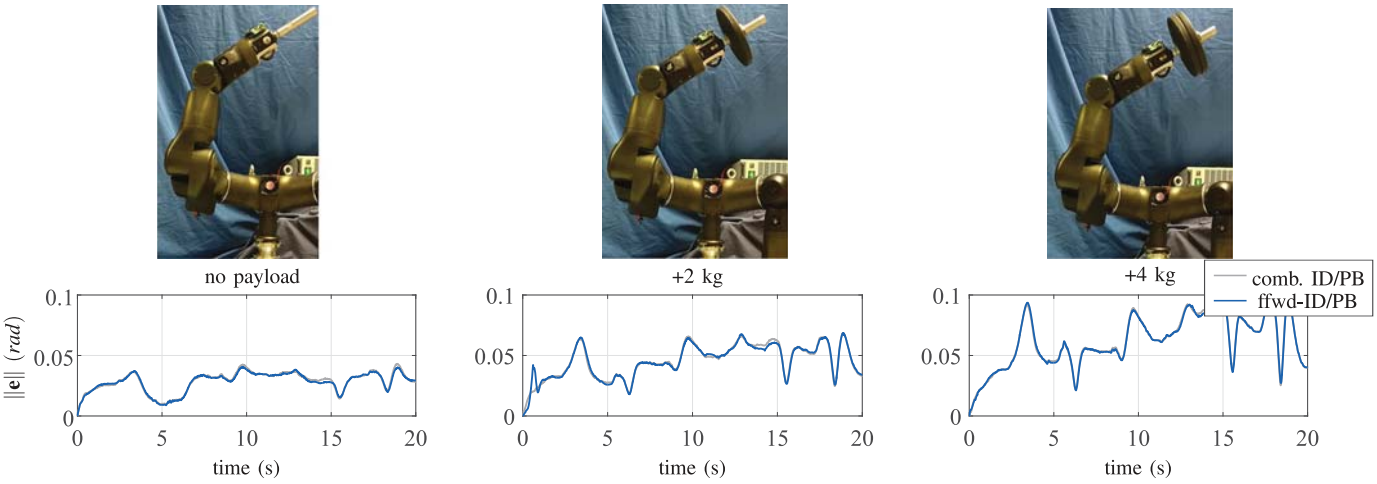

Fig. 5. Test results for trajectory tracking with different payloads. The trajectory used for this test is in the appendix.

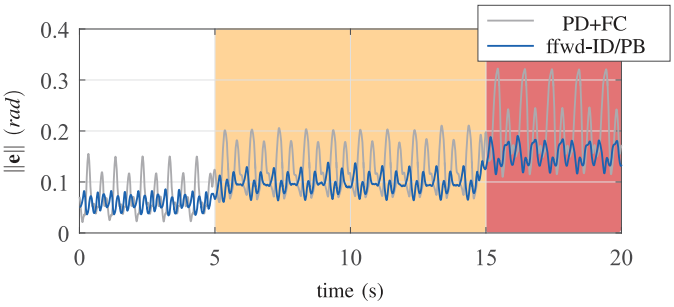

Fig. 6. Tracking test for a sawing motion with online gains reduction. Starting from the gains of the first experiment, the tuning matrix Λ is reduced during motion of 25% (orange area) and of 50% (red area). The trajectory used for this test is in the appendix.

experiment are shown in Fig. 5. In the top of this figure, the considered robot setups are shown. The test is performed for the plain robot, for a 2kg payload, and for a 4kg payload. Even when a payload differs from zero, we continue using nominal model information. Therefore, the additional contribution to the dynamics of the payloads are not present in the controller and generate a perturbation on the closed-loop system as analyzed in the previous section. Remarkably, by observing the evolution over time of the trajectory tracking errors in Fig. 5, we see good performance from both controllers, without any sign of instability and oscillations. In this case, the performance of the combined ID/PB controller and the feedforward-ID/PB are not easily distinguishable due to the relatively slow speed of the desired trajectory. In fact, when trajectories are sufficiently slow, the effect of the delay introduced by our practical approach for estimating accelerations and jerks becomes negligible. The dynamics of this trajectory has been limited to comply with the physical limits of the robot for carrying a 4kg payload reliably. The gains that we have used in this experiment are the same as those of the previous one.

In the last experiment, we show the benefit of our proposed controller with feedforward action with respect to its reduced PD version when manually reducing the gains. The reduction of the gains may be desired to obtain a task execution with low impedance. On the other hand, this would not be practical for control schemes whose tracking performance is significantly corrupted by this practice. For this test, we let the robot perform a sawing motion. In Fig. 6 we can observe that the oscillatory behavior of the error for the PD controller significantly increases when reducing the gains. From the previously mentioned gains, we decrease all entries of Λ to 50% and 25% of their original values (orange and red areas in Fig. 6, respectively). In particular, the peak-to-peak value of the oscillations raises from about 0.128 *rad* to 0.205 *rad*. In contrast, the peak-to-peak error of the feedforward-ID/PB control is not significantly affected and raises only from 0.046 *rad* to 0.065 *rad*. The reduced amplitude oscillations allow more precise movements and lead to safer conditions for letting e.g., a human establish a physical interaction with the arm. All previously discussed experiments can be seen in the video attachment. Finally, we report that the maximum total execution time of our proposed controller is about 0.14 *ms* on the available target machine.

V. Conclusions

A novel control approach for robots with elastic joints, combining the efficient implementability of classical inverse-dynamics control with the robustness of passivity-based controllers, is presented. In principle, and under reasonable assumptions, any user-defined tracking performance can be ultimately met. Of course, in practice the performance is limited due to actuator limitations (e.g., limited sampling rate, saturation, and measurement noise), which have not been considered in the theoretical analysis of this paper. However, they surely represent an interesting path to investigate for future work, together with the application on a robot arm with lower joint stiffness. Please note that we did not perform an optimization of the tracking performance (e.g., by fine tuning procedures) nor it was the scope of this paper: rather, our focus was a fair comparison among the tested schemes.

Our proposed combined ID/PB controller, together with its feedforward inverse-dynamics version has been experimentally applied with success to a 7 degrees-of-freedom robot

manipulator with mixed rigid/elastic joints. The controllers have also shown good tracking performance when a significant (unknown for the control) payload has been used. Finally, the limited degradation of the tracking performance when reducing the gains (Λ in particular) can be exploited as a useful feature for safe physical human-robot interaction tasks, since the robot can behave more compliantly.

APPENDIX A
EXPERIMENATAL TRAJECTORIES

The reference trajectories used for the experiments are a result of point-to-point motions in joint space using 7*th* order polynomials with null initial/final velocity, acceleration and jerk. The points are specified in Tab. II, III, and IV for the experiments in Fig. 6, 5, and 4, respectively.

TABLE II
SPECIFICATIONS OF THE POINT-TO-POINT MOTIONS FOR THE EXPERIMENT OF FIG. 6.

Time (s)	q_1 (rad)	q_2 (rad)	q_3 (rad)	q_4 (rad)	q_5 (rad)	q_6 (rad)	q_7 (rad)
0	$-\pi/4$	$\pi/8$	0	$\pi/2$	$\pi/6$	$\pi/4$	$-\pi/8$
0.5	$\pi/12$	$\pi/8$	0	$\pi/4$	$\pi/6$	$\pi/8$	$-\pi/8$
1	$-\pi/4$	$\pi/8$	0	$\pi/2$	$\pi/6$	$\pi/4$	$-\pi/8$
⋮	⋮	⋮	⋮	⋮	⋮	⋮	⋮
20	$\pi/12$	$\pi/8$	0	$\pi/4$	$\pi/6$	$\pi/8$	$-\pi/8$

TABLE III
SPECIFICATIONS OF THE POINT-TO-POINT MOTIONS FOR THE EXPERIMENT OF FIG. 5.

Time (s)	q_1 (rad)	q_2 (rad)	q_3 (rad)	q_4 (rad)	q_5 (rad)	q_6 (rad)	q_7 (rad)
0	0	0.1	0	0	0	0	$-\pi/8$
2	0	$\pi/8$	0	0	0	0	$-\pi/8$
5	$\pi/2$	$\pi/4$	0	$\pi/2$	$-\pi/2$	$\pi/4$	$-\pi/4$
8	$\pi/4$	$\pi/2$	$\pi/2$	$\pi/2$	$\pi/2$	$-\pi/4$	$-\pi/8$
11	$-\pi/4$	$\pi/4$	$\pi/4$	$\pi/4$	$-\pi/4$	$\pi/4$	$-\pi/4$
14	$\pi/2$	$\pi/4$	0	$\pi/8$	$\pi/4$	$-\pi/4$	$-\pi/10$
17	$\pi/2$	$\pi/2$	$\pi/2$	$\pi/2$	$\pi/4$	$\pi/4$	$-\pi/4$
20	0	$\pi/8$	0	0	0	0	$-\pi/8$

TABLE IV
SPECIFICATIONS OF THE POINT-TO-POINT MOTIONS FOR THE EXPERIMENT OF FIG. 4.

Time (s)	q_1 (rad)	q_2 (rad)	q_3 (rad)	q_4 (rad)	q_5 (rad)	q_6 (rad)	q_7 (rad)
0	0	0.1	0	0	0	0	$-\pi/8$
2	0	$\pi/8$	0	0	0	0	$-\pi/8$
4	$\pi/2$	$\pi/4$	0	$\pi/2$	$-\pi/2$	$\pi/4$	$-\pi/4$
6	$\pi/4$	$\pi/2$	$\pi/2$	$\pi/2$	$\pi/2$	$-\pi/4$	$-\pi/8$
8	$-\pi/4$	$\pi/4$	$\pi/4$	$\pi/4$	$-\pi/4$	$\pi/4$	$-\pi/4$
9	$\pi/2$	$\pi/4$	0	$\pi/8$	$\pi/4$	$-\pi/4$	$-\pi/10$
10	$\pi/2$	$\pi/2$	$\pi/2$	$\pi/2$	$\pi/4$	$\pi/4$	$-\pi/4$
11	0	$\pi/8$	0	0	0	0	$-\pi/8$

ACKNOWLEDGMENT

The research leading to these results has received funding from the People Programme (Marie Curie Actions) of the European Union's Seventh Framework Programme FP7/2007-2013/ under REA grant agreement number 608022 and the Horizon 2020 Programme under grant agreement 644839 (ICT-23-2014 Robotics).

REFERENCES

[1] A. De Santis, B. Siciliano, A. De Luca, and A. Bicchi, "An atlas of physical human-robot interaction," *Mechanism and Machine Theory*, vol. 43, no. 3, pp. 253–270, 2008.
[2] A. De Luca and W. Book, *Handbook of Robotics*. Springer, 2008, book section Robots with Flexible Elements, pp. 287–320.
[3] G. A. Pratt and M. M. Williamson, "Series elastic actuators," in *Proc. IEEE/RSJ Int. Conf. on Intelligent Robots and Systems*, vol. 1, 1995, pp. 399–406.
[4] N. G. Tsagarakis, M. Laffranchi, B. Vanderborght, and D. G. Caldwell, "A compact soft actuator unit for small scale human friendly robots," in *Proc. IEEE Int. Conf. on Robotics and Automation*, 2009, pp. 4356–4362.
[5] L. Baccelliere, N. Kashiri, L. Muratore, A. Laurenzi, M. Kamedula, A. Margan, S. Cordasco, J. Malzahn, and N. Tsagarakis, "Development of a human size and strength compatible bi-manual platform for realistic heavy manipulation tasks," in *Proc. IEEE Int. Conf. on Intelligent Robots and Systems*, 2017, pp. 5594–5601.
[6] M. W. Spong, "Control of flexible joint robots: A survey," Coordinated Science Laboratory, University of Illinois, Tech. Rep. UILU-ENG 90-2203 DC-116, 1990.
[7] A. De Luca and P. Tomei, *Theory of Robot Control*. Springer-Verlag London, 1996, ch. Elastic joints, pp. 176–217.
[8] S. Ozgoli and H. D. Taghirad, "A survey on the control of flexible joint robots," *Asian Journal of Control*, vol. 8, no. 4, pp. 332–344, 2006.
[9] M. W. Spong, "Modeling and control of elastic joint robots," *Journal of dynamic systems, measurement, and control*, vol. 109, no. 4, pp. 310–318, 1987.
[10] M. W. Spong, K. Khorasani, and P. Kokotovic, "An integral manifold approach to the feedback control of flexible joint robots," *IEEE Journal on Robotics and Automation*, vol. 3, no. 4, pp. 291–300, 1987.
[11] M. W. Spong, J. Y. Hung, S. A. Bortoff, and F. Ghorbel, "A comparison of feedback linearization and singular perturbation techniques for the control of flexible joint robots," in *Proc. American Control Conference*, 1989, pp. 25–30.
[12] A. De Luca, "Feedforward/feedback laws for the control of flexible robots," in *Proc. IEEE Int. Conf. on Robotics and Automation*, vol. 1, 2000, pp. 233–240.
[13] A. Albu-Schäffer, C. Ott, and G. Hirzinger, "A unified passivity-based control framework for position, torque and impedance control of flexible joint robots," *Int. J. Robot. Res.*, vol. 26, no. 1, pp. 23–39, 2007.
[14] A. Loría and R. Ortega, "On tracking control of rigid and flexible joints robots," *Appl. Math. Comput. Sci*, vol. 5, no. 2, pp. 101–113, 1995.
[15] B. Brogliato, R. Ortega, and R. Lozano, "Global tracking controllers for flexible-joint manipulators: a comparative study," *Automatica*, vol. 31, no. 7, pp. 941–956, 1995.
[16] S. Avila-Becerril, A. Loría, and E. Panteley, "Global position-feedback tracking control of flexible-joint robots," in *Proc. American Control Conference*, Jul. 2016, pp. 3008–3013.
[17] S. Avila-Becerril, A. Loria, and E. Panteley, "A separation principle for underactuated lossless Lagrangian systems," *IEEE Transactions on Automatic Control*, vol. 62, no. 10, pp. 5318–5323, 2017.
[18] M. Keppler, D. Lakatos, C. Ott, and A. Albu-Schäffer, "A passivity-based controller for motion tracking and damping assignment for compliantly actuated robots," in *Proc. 55th IEEE Conference on Decision and Control*, 2016, pp. 1521–1528.
[19] P. Tomei, "A simple PD controller for robots with elastic joints," *IEEE Transactions on Automatic Control*, vol. 36, no. 10, pp. 1208–1213, 1991.
[20] A. De Luca, B. Siciliano, and L. Zollo, "PD control with on-line gravity compensation for robots with elastic joints: Theory and experiments," *Automatica*, vol. 41, no. 10, pp. 1809–1819, 2005.
[21] A. De Luca and F. Flacco, "A PD-type regulator with exact gravity cancellation for robots with flexible joints," in *Proc. IEEE Int. Conf. on Robotics and Automation*, 2011, pp. 317–323.

[22] G. Buondonno and A. De Luca, "A recursive Newton-Euler algorithm for robots with elastic joints and its application to control," in *Proc. IEEE/RSJ Int. Conf. on Intelligent Robots and Systems*, 2015, pp. 5526–5532.
[23] A. Müller, "Recursive second-order inverse dynamics for serial manipulators," in *Proc. IEEE Int. Conf. on Robotics and Automation*, 2017, pp. 2483–2489.
[24] A. Giusti, J. Malzahn, N. Tsagarakis, and M. Althoff, "Combined inverse-dynamics/passivity-based control for robots with elastic joints," in *Proc. IEEE International Conference on Robotics and Automation*, 2017, pp. 5281–5288.
[25] A. De Luca and L. Ferrajoli, "A modified Newton-Euler method for dynamic computations in robot fault detection and control," in *Proc. IEEE Int. Conf. on Robotics and Automation*, 2009, pp. 3359–3364.
[26] R. Ortega, A. J. Van Der Schaft, I. Mareels, and B. Maschke, "Putting energy back in control," *IEEE Control Systems*, vol. 21, no. 2, pp. 18–33, 2001.
[27] B. Brogliato and C. C. de Wit, *Theory of Robot Control*. Springer-Verlag London, 1996, ch. Joint space control, pp. 59–114.
[28] G. Buondonno and A. De Luca, "Efficient computation of inverse dynamics and feedback linearization for VSA-based robots," *IEEE Robotics and Automation Letters*, vol. 1, no. 2, pp. 908–915, 2016.
[29] R. Ortega and M. W. Spong, "Adaptive motion control of rigid robots: a tutorial," in *Proc. 27th IEEE Conference on Decision and Control*, vol. 2, 1988, pp. 1575–1584.
[30] R. Ortega, A. Loría, P. J. Nicklasson, and H. Sira-Ramirez, *Passivity-based Control of Euler-Lagrange Systems*. Springer-Verlag London, 1998.
[31] E. Panteley, A. Loría, and A. Sokolov, "Global uniform asymptotic stability of cascaded non-autonomous non-linear systems: Application to stabilisation of a diesel engine," *European Journal of Control*, vol. 4, no. 1, pp. 107–115, 1999.
[32] E. Panteley, E. Lefeber, A. Loria, and H. Nijmeijer, "Exponential tracking control of a mobile car using a cascaded approach," *IFAC Proceedings Volumes*, vol. 31, no. 27, pp. 201–206, 1998.
[33] P. Belanger, P. Dobrovolny, A. Helmy, and X. Zhang, "Estimation of angular velocity and acceleration from shaft-encoder measurements," *Int. J. Robot. Res.*, vol. 17, no. 11, pp. 1225–1233, 1998.
[34] A. Giusti and M. Althoff, "Ultimate robust performance control of rigid robot manipulators using interval arithmetic," in *Proc. American Control Conference*, 2016, pp. 2995–3001.
[35] A. De Luca, "Decoupling and feedback linearization of robots with mixed rigid/elastic joints," *International Journal of Robust and Nonlinear Control*, vol. 8, no. 11, pp. 965–977, 1998.
[36] C. G. Atkeson, C. H. An, and J. M. Hollerbach, "Estimation of inertial parameters of manipulator loads and links," *The International Journal of Robotics Research*, vol. 5, no. 3, pp. 101–119, 1986.
[37] S. Bethge, J. Malzahn, N. Tsagarakis, and D. Caldwell, "FloBaRoID — A Software Package for the Identification of Robot Dynamics Parameters," in *Advances in Service and Industrial Robotics*, C. Ferraresi and G. Quaglia, Eds. Springer International Publishing, 2018, pp. 156–165.
[38] S. Traversaro, S. Brossette, A. Escande, and F. Nori, "Identification of fully physical consistent inertial parameters using optimization on manifolds," in *2016 IEEE/RSJ International Conference on Intelligent Robots and Systems*, 2016, pp. 5446–5451.
[39] P. R. Belanger, "Estimation of angular velocity and acceleration from shaft encoder measurements," in *Proc. IEEE Int. Conf. on Robotics and Automation*, vol. 1, 1992, pp. 585–592.

Andrea Giusti is a research fellow at Fraunhofer Italia Research, Italy and Ph.D. candidate at Technische Universität München, Germany. He received his Bachelor's Degree in Telecommunications Engineering in 2010, and his Master's Degree in Mechatronic Engineering, *summa cum laude*, in 2013, both from University of Trento, Italy. His research interests include control design, modeling, and identification of mechatronic and robotic systems.

Jörn Malzahn is a postdoctoral researcher at the Humanoid and Human Centered Mechatronics lab within the department of Advanced Robotics at the Istituto Italiano di Technologia in Genova. He received his Diploma in Electrical Engineering from TU Dortmund University in 2008 and his Ph.D. degree from the Institute of Control Theory and Systems Engineering (RST) at the same university in 2014. His research interest focuses on lightweight bioinspired structural designs in conjunction with control algorithms for robots, with the objective to improve their energy efficiency as well as strength on the one hand, while simultaneously donating sensitive proprioceptive capabilities to the robots on the other hand.

Nikos G. Tsagarakis received the D.Eng. degree in electrical and computer science engineering from the Polytechnic School of Aristotle University, Greece, in 1995, the M.Sc. degree in control engineering and the Ph.D. degree in robotics from the University of Salford, U.K. in 1997 and 2000, respectively. He is currently the Head of the Humanoid Design and Human Centered Mechatronics Lab, IIT.

Matthias Althoff is Assistant Professor in computer science at Technische Universität München, Germany. He received his Diploma Engineering Degree in Mechanical Engineering in 2005, and his Ph.D. in Electrical Engineering in 2010, both from Technische Universität München, Germany. From 2010 to 2012 he was a postdoctoral researcher at Carnegie Mellon University, Pittsburgh, USA, and from 2012 to 2013 an assistant professor at Technische Universität Ilmenau, Germany. His research interests include formal verification of continuous and hybrid systems, reachability analysis, planning algorithms, nonlinear control, robotics, automated vehicles, and power systems.